# Electronic structure and transport properties of double-stranded Fibonacci DNA

Enrique Maciá*
*Departamento de Fisica de Materiales, Facultad CC. Físicas, Universidad Complutense de Madrid, E-28040, Madrid, Spain*
(Received 19 July 2006; revised manuscript received 11 October 2006; published 5 December 2006)

We consider a class of synthetic DNA molecules based on a quasiperiodic arrangement of their constituent nucleotides. Making use of a two-step renormalization scheme the double-stranded DNA molecule is modeled in terms of a one-dimensional effective Hamiltonian, which includes contributions from the nucleobase system, the sugar-phosphate backbone, and the environment. Analytical results for the energy spectrum structure and Landauer conductance of Fibonacci DNA approximants are derived and compared with those corresponding to periodic polyGACT-polyCTGA chains. The main effect of quasiperiodic order is the emergence of a highly fragmented energy spectrum, introducing a characteristic low-energy scale in the electronic structure of aperiodic DNA chains. The presence of a series of high-conductance peaks in the transmission spectra of Fibonacci approximants indicates the existence of extended states in these systems. These results open perspectives for experimental work in nanodevices based on synthetic DNA.

DOI: 10.1103/PhysRevB.74.245105 PACS number(s): 87.14.Gg, 71.23.Ft, 71.20.−b, 73.63.−b

## I. INTRODUCTION

Nucleic acids can be classified into two broad classes: namely, duplex and single-stranded molecules of either DNA or RNA. In turn, each class can be further split into biological (i.e., samples extracted from living organisms, like viruses, bacteria, or eucaryotic cells) and artificially engineered molecules (e.g., polyG-polyC, polyA-polyT, or polyGC-polyCG chains). In general, synthetic nucleic acids considered so far comprise short oligonucleotides where relatively few base pairs (BP's) are *periodically* arranged.[1] These structures are quite different from the biological ones, in which several thousands to millions of BP's are *aperiodically* distributed, exhibiting characteristic scale-invariant properties due to the presence of long-range correlations in certain regions.[2,3] Accordingly, biological DNA exhibits a higher chemical complexity, determined by their BP sequencing. The key role of structural order in nucleic acids was earlier pointed out by Schrödinger, who introduced the notion of a one-dimensional *aperiodic crystal* in order to describe the basic structure of genetic material in the 1940s.[4] The subsequent discovery of quasicrystalline alloys, followed by the growth of different kinds of aperiodic superlattices and multilayers, based on semiconductor, dielectric, and metallic materials, have spurred interest in those arrangements of matter which exhibit a well-defined order without the recourse of periodic repetition.[5] These novel arrangements usually introduce some sort of correlation among the system building blocks, which ultimately plays a significant role in its transport properties. Thus, the study of the random dimer model,[6] originally introduced to explain the high electrical conductivity of doped polyacetylene and polyaniline, properly illustrates that, as soon as short-range dimer correlations among monomers are introduced in an otherwise random linear polymer, a significant number of extended states appear, efficiently contributing to the electrical transport.[7,8] Self-similar systems exhibiting more complex correlation patterns among their basic building blocks, like fractals or Fibonacci chains, are able to support extended electronic states as well.[9–13] Recent studies indicating the existence of well-defined currents (apparently on a micron scale) in λ-DNA molecules support the possible presence of this sort of extended states in biopolymers.[14] Although this charge carrier path is probably too large,[15] it has been theoretically shown that the presence of long-range correlations in aperiodic DNA sequences allows for efficient charge transfer over length scales up to ~100 nm.[16] In fact, experimental evidence of efficient charge transport through double-stranded (ds)DNA oligonucleotides (14–26 BP's long) with a nonperiodic nucleotide sequence has been recently reported[17,18] and the critical dependence of the measured dsDNA conductance upon the order sequence of the chain has been also demonstrated.[19]

Besides its fundamental importance for the progress of biological condensed-matter theory, several properties of biological interest may be directly related to the presence of sequence correlations in genomic DNA, including gene regulation, cell division, or damage recognition processes due to DNA-mediated charge migration.[20,21] In this sense, certain quasiperiodic systems may be regarded as useful model prototypes, able to mimic relevant features related to long-range correlation effects in natural DNA samples.[5,16] Motivated by such a possibility, some recent works have analyzed the role of quasiperiodic order in the electronic structure and charge transport efficiency of single-stranded DNA chains based on the Fibonacci polyGC sequence.[22,23] In this work, we will consider the case of more realistic dsDNA chains containing four different nucleotides, which can be arranged either periodically or quasiperiodically.

## II. DNA MODEL

Our description of electronic DNA energetics will take into account three different contributions stemming from (i) the nucleobase system, (ii) the backbone system, and (iii) the environment, as is sketched in Fig. 1. Attending to the energies involved in the different interactions, the resulting energy network can be hierarchically arranged, starting from high energy values related to the on-site energies of the bases and sugar-phosphate groups (8–12 eV),[24,25] passing through

 

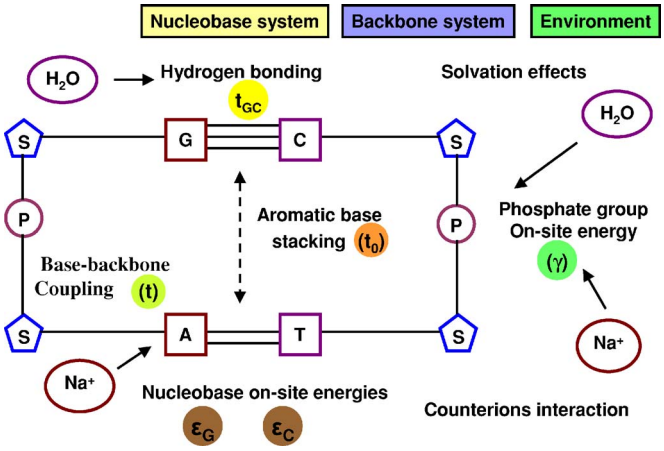


FIG. 1. (Color online) Sketch illustrating the overall energetics of a double-stranded DNA chain and the different tight-binding parameters included in the DNA model considered in this work.

intermediate energy values related to the hydrogen bonding between Watson-Crick pairs (~0.5 eV),[24,26] and the coupling between the bases and the sugar moiety (~1 eV),[25] and ending up with the aromatic base stacking low energies (0.01–0.4 eV).[24,27,28] The energy scale of environmental effects (1–5 eV) is related to the presence of counterions and water molecules, interacting with the nucleobases and the backbone by means of hydration, solvation, and charge transfer processes. It is about one order of magnitude larger than the coupling between the complementary bases and about two orders of magnitude larger than the base stacking energies.

In some previous models a transport channel associated with the possible hopping of charge carriers between successive phosphate groups along the backbone was considered.[29–31] However, first-principles calculations, showing that the phosphate molecular orbitals are systematically below the base-related ones, do not favor the presence of such a transport channel.[32,33] On the other hand, quantum mechanical studies show that hydrogen bonding interactions give rise to a spatial separation of the highest occupied and lowest unoccupied molecular orbitals (HOMO and LUMO) in the nucleobase system, so that hole (electron) transfer proceeds through the purine (pyrimidine) bases, where the HOMO (LUMO) carriers are located in polyG-polyC (polyA-polyT), respectively.[34,35] Accordingly, we shall consider that the charge transfer mainly proceeds through the aromatic base stack channel.

In Fig. 2(a) we introduce our tight-binding model for a double-stranded polyGACT-polyCTGA unit cell including four different nucleotides. This unit cell provides the basis for both periodic and aperiodic longer DNA chains, where $\varepsilon_j$, with $j=\{\mathrm{G},\mathrm{C},\mathrm{A},\mathrm{T}\}$, are the on-site energies of the bases, $t_j$ is the hopping integral between the sugar's oxygen atom and the base's nitrogen atom,[36] and $t_{GC}$ ($t_{AT}$) describes the hydrogen bonding between complementary bases. The backbone's contribution is described by means of the on-site energies $\gamma_j$, introduced in Fig. 2(b). In general, $\gamma_j$ will depend on the nature of the neighboring base as well as the presence of water molecules and/or counterions attached to the backbone, according to the overall scheme illustrated in Fig. 1. In order to obtain a simple mathematical description, keeping most of the relevant physical information, we will map the tight-binding model proposed in Fig. 2(a) onto the equivalent binary lattice model shown in Fig. 2(c). To this end, the Watson-Crick BP's are first renormalized to obtain the branched tight-binding model shown in Fig. 2(b).[37] The renormalized on-site energies and transfer integrals are, respectively, given by $\tilde{\varepsilon}_{ij}=t_{ij}$ and[38]

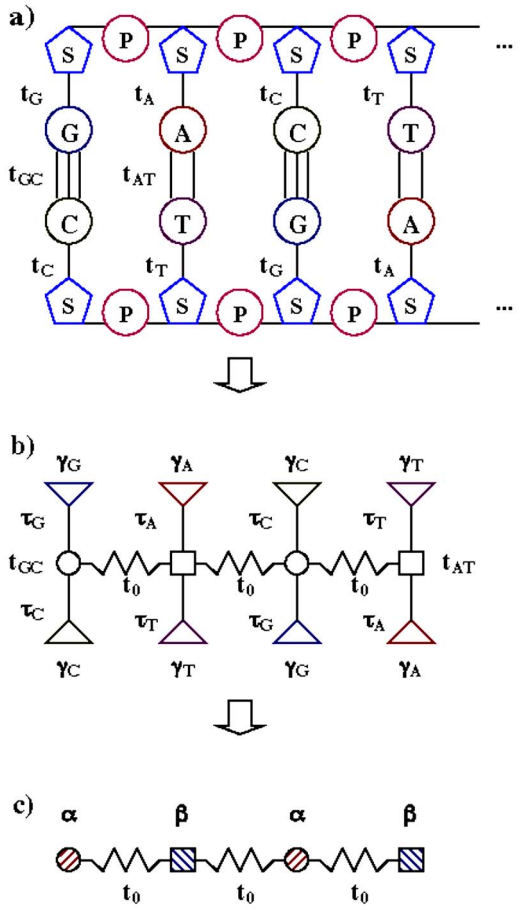


FIG. 2. (Color online) Sketch illustrating the two-step renormalization process mapping the dsDNA chain into a linear diatomic lattice. (a) Starting effective tight-binding model for the polyGACT-polyCTGA unit cell. (b) Renormalized model after the first decimation step. (c) Renormalized model after the second decimation step.

$$\tau_k = t_k + \frac{\varepsilon_k}{t_k}(E-\gamma_k). \tag{1}$$

Note that the renormalized on-site energies (given by the hydrogen bonding energy scale) are now about one order of magnitude smaller than the original ones (given by the ionization potentials of the nucleobases), so that the effective $\pi$-$\pi$ overlap integral describing the aromatic base stacking between adjacent nucleotides becomes energetically relevant and it is explicitly included in the model by means of the hopping integral $t_0$. Next, the backbone contribution is decimated to obtain the one-dimensional lattice shown in Fig.

2(c), where the renormalized on-site energies are now given by

$$\alpha,\beta = t_{\alpha,\beta} + \frac{\tau_{G,A}^2(E-\gamma_{C,T}) + \tau_{C,T}^2(E-\gamma_{G,A})}{(E-\gamma_{G,A})(E-\gamma_{C,T})}, \tag{2}$$

with $t_\alpha \equiv t_{CG}$ and $t_\beta \equiv t_{AT}$. In this way, the original polyGACT-polyCTGA chain is mapped onto the equivalent diatomic lattice shown in Fig. 2(c), where the renormalized "atoms" correspond to the Watson-Crick complementary pairs in the DNA molecule. In this way, our approach provides a more realistic description, including 15 physical parameters $\{\varepsilon_j, t_j, \gamma_j, t_{GC}, t_{AT}, t_0\}$ fully describing the energetics of the DNA molecule in terms of just three variables (i.e., $\alpha, \beta, t_0$) in a unified way.

By inspecting the renormalized binary lattice shown in Fig. 2(c) we realize that, instead of considering a periodic chain with unit cell $\alpha\beta$, we could arrange the GC and AT complementary pairs according to the Fibonacci sequence, which is prescribed by the inflation rule $\alpha \to \alpha\beta$ and $\beta \to \alpha$. In this way, we obtain the series of unit cells $\alpha\beta, \alpha\beta\alpha, \alpha\beta\alpha\alpha\beta, \alpha\beta\alpha\alpha\beta\alpha\beta\alpha, \ldots$ . The first representative in this series coincides with the periodic polyGACT-polyCTGA chain [note that, according to Eq. (2), the BP's GC/CG and AT/TA are indistinguishable in the renormalized chain]. The following terms in the sequence describe periodic DNA chains whose unit cell becomes progressively complex, attaining the quasiperiodic order characteristic of the Fibonacci sequence in the thermodynamic limit $N \to \infty$. Accordingly, the systematic study of these approximants series provides useful information regarding the progressive emergence of quasiperiodic order in the system.[39]

## III. ENERGY SPECTRUM OF THE GACT-CTGA CHAIN

Within the framework of the transfer matrix formalism and considering nearest-neighbor interactions only,[40] the Schrödinger equation of the renormalized binary chain shown in Fig. 2(c) can be expressed in terms of the following transfer matrices:

$$Q_\alpha \equiv \begin{pmatrix} 2x & -1 \\ 1 & 0 \end{pmatrix}, \quad Q_\beta \equiv \begin{pmatrix} 2y & -1 \\ 1 & 0 \end{pmatrix}, \tag{3}$$

where $x=(E-\alpha)/2t_0$ and $y=(E-\beta)/2t_0$. Assuming periodic boundary conditions the dispersion relation is given by the relationship

$$2\cos(qNa_*) = \mathrm{tr}[(Q_\beta Q_\alpha)^m] \equiv \mathrm{tr}[P_m(E)], \tag{4}$$

where $q$ is the wave vector, $N$ is the BP number, $a_*$ measures the separation between neighboring BP's along the helix axis, and $m \equiv N/2$. Since both $Q_\alpha$ and $Q_\beta$ are unimodular matrices, we can make use of the Cayley-Hamilton theorem[41] to express the global transfer matrix of the DNA chain as

$$P_m(E) = \begin{pmatrix} U_m + U_{m-1} & -2yU_{m-1} \\ 2xU_{m-1} & -U_{m-1} - U_{m-2} \end{pmatrix}, \tag{5}$$

where $U_m(z) \equiv \sin[(m+1)\theta]/\sin\theta$, with $z \equiv \frac{1}{2}\mathrm{tr}[Q_\beta Q_\alpha] \equiv \cos\theta = 2xy-1$, are Chebyshev polynomials of the second kind and we have made use of the relationship $U_{m+1} - 2zU_m + U_{m-1} = 0$. Then, taking into account the expression $(U_m - U_{m-2})/2 = \cos(m\theta)$, we finally obtain the following dispersion relation:

$$4t_0^2\cos^2(qa_0) = E^2 - (\alpha+\beta)E + \alpha\beta, \tag{6}$$

which has the typical form for a binary chain, though in this case the renormalized on-site energies $\alpha(E)$ and $\beta(E)$ explicitly depend on the charge carriers energy $E$ after Eqs. (1) and (2), leading to rather involved analytical expressions. In order to grasp the basic energy spectrum structure we will introduce two simplifications. First, according to recent x-ray experiments the counterions condense around the nucleic acid chain in a tightly bound layer.[42] Accordingly, a homogeneous charge distribution through the backbone can be assumed as a first approximation, so that $\gamma_j \equiv \gamma$. Second, the transfer integral describing the coupling between the sugar and neighbor bases takes on essentially the same values for the different nucleotides,[25] and we can confidently assume $t_j \equiv t$ as well. Thus, Eq. (2) simplifies to

$$\alpha(E) = \alpha_0 + \alpha_1 E + \frac{2t^2}{E-\gamma}, \quad \beta(E) = \beta_0 + \beta_1 E + \frac{2t^2}{E-\gamma}, \tag{7}$$

where $\alpha_0 \equiv a_0 - \gamma\alpha_1$, $\beta_0 \equiv b_0 - \gamma\beta_1$, $a_0 \equiv t_{GC} + 2(\varepsilon_G + \varepsilon_C)$, $b_0 \equiv t_{AT} + 2(\varepsilon_A + \varepsilon_T)$, $\alpha_1 \equiv (\varepsilon_G^2 + \varepsilon_C^2)/t^2$, and $\beta_1 \equiv (\varepsilon_A^2 + \varepsilon_T^2)/t^2$. Plugging Eq. (7) into Eq. (6) we obtain $(E \neq \gamma)$

$$E^4 + AE^3 + BE^2 + CE + D = 0, \tag{8}$$

where $A \equiv w - 2\gamma$, $B \equiv \xi + 2\varsigma + \gamma(\gamma - 2w)$, $C \equiv \gamma^2 w + \eta - 2\gamma(\xi + \varsigma)$, and $D \equiv 4t^4/uv + \gamma^2\xi - \gamma\eta$, and we have introduced the auxiliary variables $u \equiv \alpha_1 - 1$, $v \equiv \beta_1 - 1$, $w = \alpha_0/u + \beta_0/v$, $\eta = 2t^2(\alpha_0 + \beta_0)/uv$, $\varsigma = t^2(u^{-1} + v^{-1})$, and $\xi = [\alpha_0\beta_0 - (2t_0\cos qa_*)^2]/uv$. Therefore, though the renormalized chain only includes two "atomic" species, the energy spectrum is composed of four bands, as one expects for the tetranucleotide unit cell shown in Fig. 2(a). This result properly illustrates that the renormalized chain encompasses a full quantum description of the Watson-Crick bps energetics. The detailed structure of the energy spectrum will depend on the adopted model parameters. By considering the realistic values listed in Table I we obtain the energy spectrum shown in the left panel of Fig. 3 (for convenience the energy origin is

TABLE I. Parameters adopted for the effective Hamiltonian considered in this work arranged by decreasing energies in order to illustrate the different energy scales of relevance in the DNA system.

| Model Hamiltonian parameters (eV) | |
|---|---|
| $\varepsilon_G = 7.77$ | $\varepsilon_C = 8.87$ |
| $\varepsilon_A = 8.25$ | $\varepsilon_T = 9.13$ |
| $\gamma = 12.27$ | |
| | $t = 1.5$ |
| $t_{GC} = 0.90$ | $t_{AT} = 0.34$ |
| | $t_0 = 0.15$ |

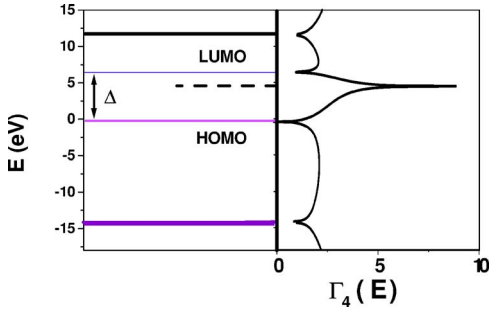


FIG. 3. (Color online) The band structure (left) and the Lyapunov exponent as a function of the energy (right) for the periodic polyGACT-polyCTGA chain derived from Eqs. (8) and (13), respectively, making use of the model parameters listed in Table I. The origin of energy is set at $\varepsilon_G$. More details in the text.

set at $\varepsilon_G$). The location of the different allowed bands and their respective bandwidths are listed in Table II. As we see, the energy spectrum consists of four narrow bands separated by wide gaps. The wide separation among the different allowed bands stems from hybridization effects between the nucleobase system and the sugar-phosphate backbone.[38] We note that the obtained bandwidths compare well with the values reported for short (5–12 BP's) polyG-polyC and polyA-polyT chains from first-principles band structure calculations (HOMO bandwidths $\simeq$50–400 meV, LUMO bandwidths $\simeq$100–300 meV).[35,43] Assuming, as it is usual, that each BP contributes one free charge carrier,[44] the HOMO band is centered at $E=-0.423$ eV, yielding a HOMO-LUMO gap width $\Delta=6.79$ eV. This figure occupies an intermediate position between numerically obtained values for polyG-polyC chains (7.4–7.8 eV) (Ref. 45) and photoemission spectroscopy measurements (4.5–5.0 eV) performed in polyG-polyC and polyA-polyT chains.[46]

The information about the overall structure of the energy spectrum obtained from the dispersion relation is complemented by the density of states (DOS), given by the following expression:[29]

$$D(E)dE = \frac{1}{N} d\left\{ \cos^{-1}\left( \frac{1}{2} \mathrm{tr}[P_m(E)] \right) \right\}, \tag{9}$$

which, according to Eq. (5), can be readily expressed as

$$D(E) = -\frac{m}{N\sqrt{1-z^2}} \frac{dz}{dE}. \tag{10}$$

TABLE II. Locations of the allowed bands centers ($E_i$), bandwidhts ($W_i$), and gap widths ($\Delta_{ij}$) in the energy spectrum corresponding to the polyGACT-polyCTGA chain.

| Band center (eV) | Bandwidth (meV) | Gap width (eV) |
|---|---|---|
| $E_1=-14.209$ | $W_1=269$ | |
| $E_2=-0.423$ | $W_2=120$ | $\Delta_{12}=13.591$ |
| $E_3=+6.440$ | $W_3=29$ | $\Delta=6.788$ |
| $E_4=+11.595$ | $W_4=177$ | $\Delta_{34}=5.052$ |

From the definition of the variables $z$, $x$, and $y$, and Eq. (7), one finally obtains

$$D(E) = \frac{yu + xv - 2t^2(x+y)(E-\gamma)^{-2}}{4t_0\sqrt{xy(1-xy)}}. \tag{11}$$

Due to the one-dimensional nature of the considered model, the obtained DOS is characterized by a number of sharp features (van Hove singularities) given by the conditions $E=\alpha$, $E=\beta$, and $4t_0^2=(E-\alpha)(E-\beta)$, which determine the allowed band-edge positions. In addition, we also have a resonant feature at $E=\gamma$. This resonance is a characteristic signature of the sugar-phosphate subsystem, which is shown as a dashed line in the left panel of Fig. 3.

The system transport properties are related to the localization degree of the different states belonging to the spectrum. The Lyapunov coefficient, defined by the expression[47,48]

$$\Gamma(E) = \lim_{N\to\infty} \Gamma_N(E) = \lim_{N\to\infty} \frac{1}{2N} \ln(\mathrm{tr} P_N P_N^{\dagger}), \tag{12}$$

where $P^{\dagger}$ denotes the Hermitian conjugate of $P$, provides the growth ratio of the wave function for an eigenstate of energy $E$ along the system. Gaps in the energy spectrum are characterized by maxima of $\Gamma$, whereas allowed bands correspond to minima of $\Gamma$. In particular, when considering extended states belonging to the allowed bands of periodic systems one gets $\Gamma(E)=0$. In the case of exponentially localized eigenstates this property is not fulfilled and the value of the Lyapunov coefficient provides a measure of the localization length $\xi$ of the considered state through the relationship $\xi(E)=\Gamma^{-1}(E)$.

Plugging the matrix elements given by Eq. (5) into Eq. (12) we obtain

$$\Gamma(E) = \lim_{m\to\infty} \frac{1}{4m} \ln\{2 + 4U_{m-1}^2[4x^2y^2 + (x-y)^2]\}. \tag{13}$$

The length dependence of the logarithm appearing in Eq. (13) is determined by the Chebyshev polynomials $U_{m-1}(z)$, which remain always bounded for $E\neq\gamma$. Accordingly, one gets $\Gamma(E)\to 0$ in the thermodynamic limit, hence indicating the extended nature of these eigenstates. This result is properly illustrated in the right panel of Fig. 3, where we clearly appreciate the correlation between small Lyapunov coefficient values and the presence of allowed bands. We also note the presence of a localized state corresponding to the resonant state $E=\gamma$. In this case, the product $xy$ diverges in Eq. (13), so that we obtain $\Gamma(E)\to\infty$ [i.e., $\xi(E)\to 0$]. The resonant state $E=\gamma$ is determined by the backbone on-site energies, which, in turn, depend on environmental effects due to solvation and hydration processes involving the cations and the water shell (see Fig. 1). Therefore, our simplified Hamiltonian model is able of including the existence of localized states in the HOMO-LUMO gap stemming from environmental effects, in agreement with previous results obtained from detailed *ab initio* calculations.[32,49] In this regard, we note that the number of resonant localized states within the gap region will be increased by properly relaxing the condition $\gamma_j \equiv \gamma$ in our treatment.

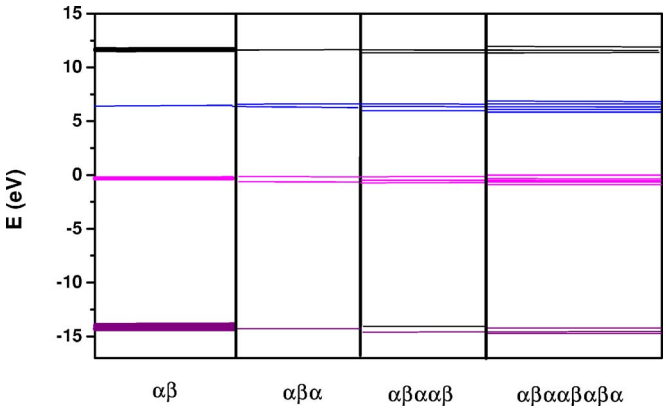


FIG. 4. (Color online) The energy specta of successive approximants of the Fibonacci DNA chain, obtained from Eqs. (14), are compared to that corresponding to the polyGACT-polyCTGA chain. The model parameters are listed in Table I.

## IV. ENERGY SPECTRA OF FIBONACCI APPROXIMANTS

Following the approach introduced in the previous section the dispersion relations of a successive series of approximants can be obtained from the knowledge of the corresponding global transfer matrices, respectively given by $Q_\alpha Q_\beta Q_\alpha$, $Q_\beta Q_\alpha Q_\alpha Q_\beta Q_\alpha$, and so on. For instance, for the $\alpha\beta\alpha$, $\alpha\beta\alpha\alpha\beta$, and $\alpha\beta\alpha\alpha\beta\alpha\beta\alpha$ approximants, we respectively obtain

$$2x(2xy-1)-y=\cos(3qa_*),$$

$$4yx(4x^2y-4x-y)+3x+2y=\cos(5qa_*),$$

$$8yx\{8yx[yx(2x^2-1)-3x^2+1]+11x^2+y^2-2\}-12x^2-4y^2+1=\cos(8qa_*). \quad (14)$$

The corresponding spectra are shown in Fig. 4. By inspecting this figure we see that the four bands originally present in the energy spectrum of the polyGACT-polyCTGA chain become progressively fragmented as we consider successive approximants. Thus, the two central bands in the energy spectrum of the $\alpha\beta$ chain split into two subbands in the energy spectrum of the $\alpha\beta\alpha$ approximant, into three subbands in the energy spectrum of the $\alpha\beta\alpha\alpha\beta$ approximant, and into five subbands in the energy spectrum of the $\alpha\beta\alpha\alpha\beta\alpha\beta\alpha$ approximant. As we see, this fragmentation scheme follows the series {1, 2, 3, 5,…} subbands. In a similar way, we see that the edge bands in the energy spectrum of the $\alpha\beta$ chain follow the fragmentation scheme {1, 1, 2, 3,…} subbands. In both cases the fragmentation scheme is described by the Fibonacci series $F_n=\{1,1,2,3,5,8,\ldots\}$, which is obtained from the recursion expression $F_{n+1}=F_n+F_{n-1}$, with $F_0=F_1=1$. Thus, the total number of subbands composing the spectrum of a given approximant can be expressed as $2F_{\nu-1}+2F_{\nu-2}=2F_\nu$, where $\nu$ is the number of Watson-Crick BP's contained in the approximant unit cell. This kind of highly fragmented energy spectrum is a typical feature of quasiperiodic systems[5] and gives rise to the presence of two different energy scales in the DNA spectrum. On the one hand, we have a large energy scale (within the range 5–14 eV) determined by the width of the gaps among the main bands. On the other hand, due to the progressive fragmentation of these main bands, an increasing number of narrow gaps progressively appear in the spectra of higher-order approximants. In this way, the emergence of the quasiperiodic order naturally introduces a specific, small energy scale in the DNA electronic structure, ranging from about 0.1–0.5 eV for the low-order $\alpha\beta\alpha\alpha\beta$ approximant to values well below 100 meV for higher-order approximants. The presence of these small activation energies in the electronic structure brings an additional mechanism in order to explain the anomalous absorption feature observed at low (10–100 meV) energies in optical conductivity spectra of biological DNA samples.[50]

What is the nature of the states belonging to this highly fragmented spectra? From a physical viewpoint, the states can be classified according to their transport properties which, in turn, are determined by the spatial distribution of the wave function amplitudes. Thus, conducting, crystalline systems are described by periodic Bloch states, whereas insulating systems are described by exponentially decaying wave functions corresponding to localized states. For systems described in terms of Fibonacci on-site Hamiltonians it has been rigorously proven that the energy spectrum is singularly continuous and the amplitudes of its eigenstates do not tend to zero at infinity but are bounded below throughout the system,[51] yielding the value $\Gamma(E)=0$ in the thermodynamic limit.[47] This result also holds for the Fibonacci DNA chain we are considering in this work. In fact, from Eq. (12) we obtain

$$\Gamma(E)=\lim_{m\to\infty}\frac{1}{6m}\ln[2+4U_{m-1}^2P(x,y)]\to 0, \quad \forall\, E\neq\gamma, \quad (15)$$

for the $\alpha\beta\alpha$ approximant, where $P(x,y)\equiv 1+2y(y-1)+4xy(3xy+y-2)$. For higher-order approximants similar expressions are obtained, each one characterized by a corresponding $P(x,y)$ function multiplied by the bounded Chebyshev polynomial $U_{m-1}^2$. Nevertheless, the vanishing of the Lyapunov exponent should not be naively interpreted as indicating a Block-like nature for the electronic states. In most quasiperiodic systems we have critical wave functions whose amplitudes are roughly modulated by scaling exponents $\beta$ describing a power-law behavior of an envelope as $|\psi_n|\simeq|n-n_k|^{-\beta}$, so that a set of exponents $\beta_n$ (rather than a single localization length parameter) is usually required to properly characterize the nature of these eigenstates,[52] although one may reasonably expect their related transport properties to be more similar to those corresponding to extended states than to localized ones.[10–12] In Fig. 5 we illustrate the progressive fragmentation of the energy spectrum around the energy value $E\simeq -0.4$ eV for increasing-order Fibonacci DNA approximants. As we can see, a self-similar, nested structure, characteristic of the long-range quasiperiodic order present in Fibonacci systems, progressively appears in the Lyapunov coefficient overall structure as the complexity of the corresponding unit cell is increased for successive approximants.

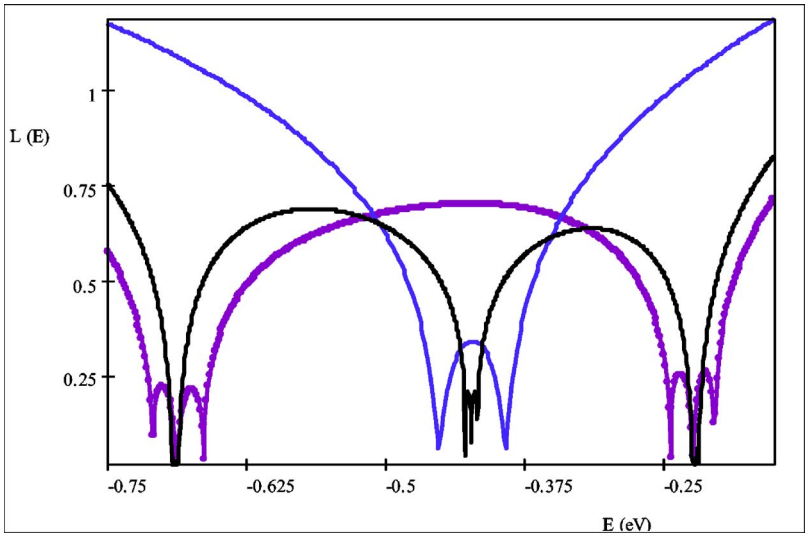


FIG. 5. (Color online) Lyapunov coefficient as a function of the energy for successive approximants of the Fibonacci DNA chain containing $N=6$ BP's (three $\alpha\beta$ unit cells, solid gray), $N=12$ BP's (four $\alpha\beta\alpha$ unit cells, dotted curve), and $N=20$ BP's (four $\alpha\beta\alpha\alpha\beta$ unit cells, solid black).

## V. LANDAUER CONDUCTANCE AND TRANSMISSION SPECTRA

In order to ascertain the *intrinsic* DNA electrical transport properties, one must pay particular attention to the role of contacts.[53] On the one hand, transport experiments have shown that chemical bonding between DNA and metal electrodes is a prerequisite for achieving reproducible conductivity results.[32,54–57] On the other hand, if the contact bonding is too strong, we should consider the states belonging to the coupled molecular-metallic system rather than those of the molecular subsystem alone.[58] Fortunately, in the DNA-metal junction case, one can consider the weak-coupling limit.[32,53] Accordingly, the effective Hamiltonian describing the ds-DNA in between two metallic leads will be written as[59,60]

$$\mathcal{H} = \sum_{n=1}^{N} (\tilde{\varepsilon}_n c_n^\dagger c_n - t_0 c_n^\dagger c_{n+1} + \text{H.c.}) - \tau(c_0^\dagger c_1 + c_{N+1}^\dagger c_N + \text{H.c.}) + \sum_{k=0}^{-\infty} (\varepsilon_M c_k^\dagger c_k - t_M c_k^\dagger c_{k+1} + \text{H.c.}) + \sum_{k=N+1}^{+\infty} (\varepsilon_M c_k^\dagger c_k - t_M c_k^\dagger c_{k+1} + \text{H.c.}), \tag{16}$$

where $c_s^\dagger$ ($c_s$) is the creation (annihilation) operator for a charge at the $s$th site in the chain. The first term describes the charge carrier propagation through the DNA chain in terms of the renormalized variables $\tilde{\varepsilon}_n=\{\alpha(E),\beta(E)\}$ and $t_0$. The second term describes the DNA-metal contacts, where $\tau$ measures the coupling strength between the leads and the end nucleotides, and the last two terms describe the metallic leads at both sides of the DNA chain, modeled as semi-infinite one-dimensional chains of atoms with one orbital per site, where $\varepsilon_M$ is the on-site energy and $t_M$ is the hopping term.

In the absence of any applied voltage the fraction of tunneling electrons transmitted through a DNA chain of length $N$ is given by the energy-dependent transmission coefficient $T_N(E)$, which is related to the the Landauer conductance $G(E)=G_0T_N(E)$, where $G_0\equiv 2e^2/h\simeq 12\,906^{-1}\ \Omega^{-1}$ is the conductance quantum. The transmission coefficient can be obtained from knowledge of the lead dispersion relation $E=\varepsilon_M+2t_M\cos k$ and the matrix elements of the metal-DNA-metal transfer matrix $\mathcal{M}_N(E)=L_N\bar{Q}^{m-1}L_1$, where the contact matrices

$$L_1=\begin{pmatrix} 2x & -\lambda \\ 1 & 0 \end{pmatrix}, \quad L_N=\lambda^{-1}\begin{pmatrix} 2y & -1 \\ \lambda & 0 \end{pmatrix}$$

describe the coupling between the DNA and metallic leads in terms of the coupling strength $\lambda\equiv\tau/t_0$. For the periodic polyGACT-polyCTGA chain $\bar{Q}=Q_\alpha Q_\beta$, and one gets

$$\mathcal{M}_N(E)=\begin{pmatrix} \lambda^{-1}(U_m+U_{m-1}) & -2yU_{m-1} \\ 2xU_{m-1} & -\lambda(U_{m-1}+U_{m-2}) \end{pmatrix}.$$

Making use of the relationship $U_{m-1}^2-U_mU_{m-2}=1$, it is easy to check that $\det[\mathcal{M}_N(E)]=1$. The transmission coefficient is then given by the relationship $T_N(E)=4\sin^2 k/\mathcal{D}_N(E)$, where[61]

$$\mathcal{D}_N(E)=[M_{12}-M_{21}+(M_{11}-M_{22})\cos k]^2 + (M_{11}+M_{22})^2\sin^2 k. \tag{17}$$

Taking into account the relationship $U_m^2+U_{m-1}^2-2zU_mU_{m-1}=1$, after some algebra one gets the following expression for the Landauer conductance:

$$G_m(E)=G_0\left\{1+(x-y)^2U_{m-1}^2 + t_M^2\frac{[f_\lambda(E,U_m)-2(x+y)U_{m-1}\cos k]^2}{(E-E_-)(E_+-E)}\right\}^{-1}, \tag{18}$$

where the auxiliary function $f_\lambda(E,U_m)\equiv\lambda^{-1}(U_{m-1}+U_m)+\lambda(U_{m-2}+U_{m-1})$ describes contact effects[53] and $E_\pm=\varepsilon_M\pm 2t_M$ define the allowed spectral window as determined by the metallic lead bandwidth. The term $(x-y)^2U_{m-1}^2$ in Eq. (18) accounts for the chemical diversity

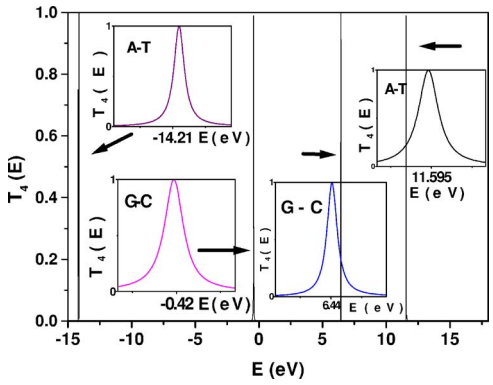


FIG. 6. (Color online) Transmission coefficient as a function of the energy for a periodic polyGACT-polyCTGA chain with $N=4$ BP's.

of a polyGACT-polyCTGA chain as compared to either polyG-polyC or polyA-polyT chains, and its main physical effect is to reduce the overall conductance of the former with respect to that obtained for the simpler ones. In Fig. 6, the energy dependence of the transmission coefficient is shown as a function of the injected charges energy at zero bias. In the insets the transmission band profile is magnified. As we see, the full transmission condition is fulfilled for all four bands, indicating the extended nature of their eigenstates. By taking $y=x$ in Eq. (18) we can obtain the transmission spectra for the polyG-polyC chain (the expression for polyA-polyT is then obtained by simply replacing $x \rightarrow y$). In this way, we can assign the central bands in the energy spectrum to GC BP's, while the edge bands in the spectrum are related to the AT BP's. Since the central bands are closer to the adopted Fermi energy, we conclude that the charge transfer will be dominated by the HOMO band in the considered system, so that it will exhibit a $p$-type behavior.

The Landauer conductance of the DNA Fibonacci approximants is obtained in an analogous way, and it can be expressed in the general form

$$G_m(E) = G_0 \left\{ 1 + C(x,y) U_{m-1}^2 + t_M^2 \frac{[F_\lambda(E, U_{m-1}) - Q(x,y) U_{m-1} \cos k]^2}{(E - E_-)(E_+ - E)} \right\}^{-1}, \tag{19}$$

where the auxiliary functions $F_\lambda$, $C$, and $Q$ are characteristic of each approximant. In order to understand the intrinsic transport properties of the Fibonacci DNA chains we will first focus on the simpler case $\lambda=1$, hence neglecting contact effects as a first approximation.[62] In that case, Eq. (19) can be expressed as

$$G_m(E) = G_0 \left\{ 1 + \left[ C(x,y) + 4t_M^2 \frac{[F(x,y) - Q(x,y)\cos k]^2}{(E - E_-)(E_+ - E)} \right] U_{m-1}^2 \right\}^{-1}. \tag{20}$$

We note that at the allowed band edges [which according to the dispersion relation are determined from the condition $\cos(m\theta) = \pm 1$] we get $U_{m-1}=0$ and the full transmission condition $T_m=1$ is satisfied. In this way, the transmission spectrum is characterized by a series of $G_0$ conductance peaks, hence confirming the extended nature of the eigenstates belonging to the different allowed bands in the Fibonacci approximants. On the other hand, as soon as contact effects are explicitly included in Eq. (19), the condition $U_{m-1}=0$ (which implies $U_m = -U_{m-2} = 1$) leads to

$$G_m(E) = G_0 \left\{ 1 + \left( \frac{1-\lambda^2}{\lambda} \right)^2 \frac{t_M^2}{(E - E_-)(E_+ - E)} \right\}^{-1} < G_0, \tag{21}$$

so that the transmission peaks do not reach in general the full transmission condition. We remark that this transmission degradation is then a direct consequence of contact effects, masking the fact that the electronic eigenstates are actually extended ones [i.e, $\Gamma(E)=0$]. This result properly illustrates the inherent difficulty in extracting reliable information concerning the nature of the conducting states from transport measurements performed in DNA chains.

## VI. CONCLUSIONS

First-principles calculations are an excellent tool for a complete characterization of the structural and electronic properties of different molecules. However, the complexity of double-stranded DNA molecule makes this method very time consuming and most studies have been restricted to consideration of short DNA oligomers containing 4–11 BP's. Consequently, model Hamiltonian approaches offer an efficient complementary way to study electronic properties and charge transport in DNA chains.[63,64] In this work we have introduced a tight-binding model able of describing both periodic and aperiodic dsDNA chains in terms of a renormalized effective lattice model entailing substantial physicochemical information concerning nucleotide interactions and backbone effects. In this way, our approach provides a realistic description of the dsDNA electronic structure, fully describing its basic energetics in terms of just three variables (i.e., $\alpha, \beta, t_0$) in a unified way. The reliability of this model has been tested by considering a periodic polyGACT-polyCTGA chain, arriving at the following main results: (i) the obtained bandwidths compare well with those reported from first-principles band structure calculations,[35,43] (ii) the obtained HOMO-LUMO band gap compares reasonably well with the values reported from both numerical and experimental studies of synthetic DNA chains,[45,46] and (iii) the existence of localized states in the HOMO-LUMO gap stemming from environmental effects is also predicted, in agreement with previous detailed *ab initio* calculations.[32,49] Accordingly, we conclude that our proposed effective Hamiltonian model provides a useful approach to describe the main electronic structure features of double-stranded, synthetic DNA molecules.

The study of the polyGACT-polyCTGA molecule paves the way towards the study of more complex DNA molecules

of biological interest, differing in size, chemical complexity, and the kind of structural order. From general principles one would expect that the nonperiodic nature of their nucleotide sequence distribution will favor localization of charge carriers in biological nucleic acids, reducing the charge transfer rate due to backscattering effects.[65] Nevertheless, this scenario must be refined in order to take into account correlation effects among nucleotides reported in biological DNA samples, since these correlations can enhance charge transport via resonant effects.[16,22,66,67] As a suitable example in this work we present a detailed analytical study of the electronic structure and Landauer conductance of short double-stranded DNA chains where the Watson-Crick BP's are arranged according to the Fibonacci series. To the best of our knowledge these sort of Fibonacci dsDNA molecules have not been previously considered in the literature, though I understand that they may be easily synthesized with current biotechnological techniques. From our study we conclude that the emergence of quasiperiodic order naturally introduces a specific, small energy scale in the DNA electronic structure, ranging from about 0.1–0.5 eV for the low-order $\alpha\beta\alpha\alpha\beta$ approximant to values well below 100 meV for higher-order approximants. The presence of these small activation energies in the electronic structure, along with the presence of a conductance peak series in the transmission spectra, suggests the possible presence of some specific features in their related transport properties, which may be eventually related to the anomalous behavior observed in optical conductivity spectra of biological DNA samples.[50]

Certainly, the possible observation of these small-energy-scale features crucially depends on the robustness of the electronic structure finer details against thermal effects. Taking the amount $k_BT \simeq 26$ meV as a suitable reference value for thermal energy at room temperature, we realize that our description should be restricted to the low-temperature regime, especially in the case of higher-order Fibonacci DNA approximants. In addition, when temperature effects are explicitly taken into account a broad collection of additional transport mechanisms can be present, such as activated hole transport[68] (including variable-range hopping),[69] phonon-assisted polaron hopping[70–72] (including large molecular rotations effects,[73] as well as disorder effects related to both the base sequence and the counterions distribution),[74] or ionic conduction due to the counterions.[70] Accordingly, the existence of extended states should not be considered as a prerequisite for efficient transport along DNA at relatively high temperatures.

## ACKNOWLEDGMENTS

I warmly thank E. Artacho, R. Gutiérrez, S. Roche, and E. B. Starikov for sharing useful information. I acknowledge M. V. Hernández for a critical reading of the manuscript. This work has been supported by the Universidad Complutense de Madrid through Project No. PR27/05-14014-BSCH.

*Electronic address: emaciaba@fis.ucm.es

[1] T. Kawai and M. Taniguchi, Physica E (Amsterdam) **33**, 1 (2006).
[2] C. K. Peng, S. V. Buldyrev, A. L. Goldberger, S. Havlin, F. Sciortino, M. Simons, and H. E. Stanley, Nature (London) **356**, 168 (1992).
[3] R. F. Voss, Phys. Rev. Lett. **68**, 3805 (1992); A. Arneodo, E. Bacry, P. V. Graves, and J. F. Muzy, *ibid.* **74**, 3293 (1995); B. Audit, C. Thermes, C. Vaillant, Y. d'Aubenton-Carafa, J. F. Muzy, and A. Arneodo, *ibid.* **86**, 2471 (2001).
[4] E. Schrödinger, *What is Life? The Physical Aspects of the Living Cell* (Cambridge University Press, New York, 1945).
[5] E. Maciá, Rep. Prog. Phys. **69**, 397 (2006).
[6] P. Phillips and H. L. Wu, Science **252**, 1805 (1991).
[7] A. Sánchez, E. Maciá, and F. Domínguez-Adame, Phys. Rev. B **49**, 147 (1994).
[8] P. Carpena, P. B. Galván, P. Ch. Ivanov, and H. E. Stanley, Nature (London) **418**, 955 (2002); Nature (London) **421**, 764 (2003).
[9] E. Maciá, Phys. Rev. B **57**, 7661 (1998).
[10] E. Maciá and F. Domínguez-Adame, Phys. Rev. Lett. **76**, 2957 (1996).
[11] V. Kumar, J. Phys.: Condens. Matter **2**, 1349 (1990).
[12] A. Chakrabarti, S. N. Karmakar, and R. K. Moitra, Phys. Lett. A **168**, 301 (1992); Phys. Rev. B **50**, 13276 (1994); S. Sil, S. N. Karmakar, R. K. Moitra, and A. Chakrabarti, *ibid.* **48**, 4192 (1993).
[13] R. Oviedo-Roa, L. A. Pérez, and C. M. Wang, Phys. Rev. B **62**, 13805 (2000); V. Sánchez and C. M. Wang, *ibid.* **70**, 144207 (2004).
[14] S. Nakamae, M. Cazayous, A. Sacuto, P. Monod, and H. Bouchiat, Phys. Rev. Lett. **94**, 248102 (2005).
[15] E. B. Starikov, Phys. Rev. Lett. **95**, 189801 (2005); S. Nakamae, M. Cazayous, A. Sacuto, P. Monod, and H. Bouchiat, *ibid.* **95**, 189802 (2005); K. Mizoguchi, S. Tanaka, and H. Sakamoto, *ibid.* **96**, 089801 (2006); S. Nakamae, M. Cazayous, A. Sacuto, P. Monod, and H. Bouchiat, *ibid.* **96**, 089802 (2006).
[16] S. Roche, D. Bicout, E. Maciá, and E. Kats, Phys. Rev. Lett. **91**, 228101 (2003); S. Roche, D. Bicout, E. Maciá, and E. Kats, *ibid.* **92**, 109901(E) (2004).
[17] H. Cohen, C. Nogues, R. Naaman, and D. Porath, Proc. Natl. Acad. Sci. U.S.A. **102**, 11589 (2005).
[18] B. Xu, P. M. Zhang, X. L. Li, and N. J. Tao, Nano Lett. **4**, 1105 (2004).
[19] J. Hihath, B. Xu, P. M. Zhang, and N. J. Tao, Proc. Natl. Acad. Sci. U.S.A. **102**, 16979 (2005).
[20] E. Braun, Y. Eichen, U. Sivan, and G. Ben-Yoseph, Nature (London) **391**, 775 (1998).
[21] C. Treadway, M. G. Hill, and J. K. Barton, Chem. Phys. **281**, 409 (2002).
[22] S. Roche and E. Maciá, Mod. Phys. Lett. B **18**, 847 (2004).
[23] B. P. W. de Oliveira, E. L. Albuquerque, and M. S. Vasconcelos, Surf. Sci. **600**, 3770 (2006).
[24] Y. J. Yan and H. Zhang, J. Theor. Comput. Chem. **1**, 225 (2002).
[25] K. Iguchi, Int. J. Mod. Phys. B **18**, 1845 (2004).

[26] The precise nature of hydrogen bonding in Watson-Crick BP's has been the subject of a number of recent quantum chemistry studies indicating that the orbital interaction accounts for about 40% and the electrostatic attraction about 60% of all attractive forces, C. Fonseca Guerra, F. M. Bickelhaupt, and E. J. Baerends, Cryst. Growth Des. **2**, 239 (2002). Taking the value 25 kcal/mol for the G-C energy coupling, the figure corresponding to the orbital overlapping yields $t_{GC} \simeq 0.4$ eV. This transfer integral value is significantly larger than that reported from first-principles band structure calculations for guanine ribbons, A. Calzolari, R. Di Felice, E. Molinari E, and A. Garbesi, Physica E (Amsterdam) **13**, 1236 (2002).

[27] T. Natsume, K. Dedachi, S. Tanaka, T. Higuchi, and N. Kurita, Chem. Phys. Lett. **408**, 381 (2005).

[28] H. Sugiyama and I. Saito, J. Am. Chem. Soc. **118**, 7063 (1996); A. A. Voityuk, J. Jortner, M. Bixon, and N. Rösch, J. Chem. Phys. **114**, 5614 (2001).

[29] K. Iguchi, J. Phys. Soc. Jpn. **70**, 593 (2001); Int. J. Mod. Phys. B **11**, 2405 (1997).

[30] H. Yamada, Int. J. Mod. Phys. B **18**, 1697 (2004).

[31] G. Xiong and X. R. Wang, Phys. Lett. A **344**, 64 (2005).

[32] R. G. Endres, D. L. Cox, and R. R. P. Singh, Rev. Mod. Phys. **76**, 195 (2004).

[33] M. S. Xu, R. G. Endres, S. Tsukamoto, M. Kitamura, S. Ishida, and Y. Arakawa, Small **1**, 1168 (2005).

[34] E. B. Starikov, Philos. Mag. **85**, 3435 (2005).

[35] E. Artacho, M. Machado, D. Sánchez-Portal, P. Ordejón, and J. M. Soler, Mol. Phys. **101**, 1587 (2003).

[36] According to quantum calculations reported by M. Unge and S. Stafström [Nano Lett. **3**, 1417 (2003)], the orbital overlapping between the sugar carbon and nucleobase nitrogen atoms forming the glycosidic bond is almost negligible for G-sugar and A-sugar nucleosides. In the case of C-sugar and T-sugar moieties such overlapping gives rise to a small shift of the on-site base energies of about 0.12 eV.

[37] The topological structure of the renormalized chain shown in Fig. 2(b) coincides with the Fishbone model discussed by G. Cuniberti, L. Craco, D. Porath, and C. Dekker, Phys. Rev. B **65**, 241314(R) (2002) and D. Klotsa, R. A. Römer, and M. S. Turner, Biophys. J. **89**, 2187 (2005), but in our model the renormalized parameters $\tilde{\varepsilon}$ and $\tau_j$ entail substantial physicochemical information concerning nucleotide interactions and backbone gating effects.

[38] E. Maciá and S. Roche, Nanotechnology **17**, 3002 (2006).

[39] E. Maciá, F. Domínguez-Adame, and A. Sánchez, Phys. Rev. B **49**, 9503 (1994).

[40] A comparison between density functional calculations and a tight-binding model, reported in Ref. 36, indicates that second-nearest-neighbor interactions are one order of magnitude smaller than nearest-neighbor ones. A detailed numerical study on the interbase coupling in ds B-DNA structures containing 4–8 BP's concluded that the hopping integrals beyond second-nearest-neighbor bases are negligible [H. Mehrez and M. P. Anantram, Phys. Rev. B **71**, 115405 (2005)].

[41] Let $\mathbf{A}$ be a matrix belonging to the $\mathrm{SL}(2,\mathbb{R})$ group. Then, $\mathbf{A}^n = U_{n-1}(z)\mathbf{A} - U_{n-2}(z)\mathbf{I}$, where $U_k(z)$ is a Chebyshev polynomial of the second kind and $z \equiv \mathrm{tr}\mathbf{A}/2$. For an elegant derivation of this result the reader is referred to D. J. Griffiths and C. A. Steinke, Am. J. Phys. **69**, 137 (2001).

[42] K. Andresen, R. Das, H. Y. Park, H. Smith, L. W. Kwok, J. S. Lamb, E. J. Kirkland, D. Herschlag, K. D. Finkelstein, and L. Pollack, Phys. Rev. Lett. **93**, 248103 (2004); R. Das, T. T. Mills, L. W. Kwok, G. S. Maskel, I. S. Millet, S. Doniach, K. D. Finkelstein, D. Herschlag, and L. Pollack, *ibid.* **90**, 188103 (2003).

[43] J. P. Lewis, P. Ordejón, and O. F. Sankey, Phys. Rev. B **55**, 6880 (1997); P. J. de Pablo, F. Moreno-Herrero, J. Colchero, J. Gomez-Herrero, P. Herrero, A. M. Baro, P. Ordejón, J. M. Soler, and E. Artacho, Phys. Rev. Lett. **85**, 4992 (2000); Ch. Adessi and M. P. Anantram, Appl. Phys. Lett. **82**, 2353 (2003); Ch. Adessi, S. Walch, and M. P. Anantram, Phys. Rev. B **67**, 081405(R) (2003); H. Wang, J. P. Lewis, and O. F. Sankey, Phys. Rev. Lett. **93**, 016401 (2004).

[44] The electrical conductance of both periodic and aperiodic DNA molecules with varied density of charge carriers has been recently discussed by X. Gao, X. Fu, L. M. Mei, and S. J. Xie, J. Chem. Phys. **124**, 234702 (2006).

[45] D. M. York, T. S. Lee, and W. Yang, Phys. Rev. Lett. **80**, 5011 (1998).

[46] H. S. Kato, M. Furukawa, M. Kawai, M. Taniguchi, T. Kawai, T. Hatsui, and N. Kosugi, Phys. Rev. Lett. **93**, 086403 (2004); H. Wadat, K. Okazaki, Y. Niimi, A. Fujimori, H. Tabata, J. Pikus, and J. P. Lewis, Appl. Phys. Lett. **86**, 023901 (2005).

[47] A. Sütö, in *Beyond Quasicrystals*, edited by F. Axel and D. Gratias (Les Editions de Physique, Les Ulis, 1995), p. 483; A. Sütö, J. Stat. Phys. **56**, 525 (1989).

[48] K. Iguchi, J. Math. Phys. **35**, 1008 (1994).

[49] F. L. Gervasio, P. Carloni, and M. Parrinello, Phys. Rev. Lett. **89**, 108102 (2002).

[50] A. Hübsch, R. G. Endres, D. L. Cox, and R. R. P. Singh, Phys. Rev. Lett. **94**, 178102 (2005); E. Helgren, A. Omerzu, G. Grüner, D. Mihailovic, R. Podgornik, and H. Grimm, cond-mat/0111299 (unpublished).

[51] B. Iochum and D. Testard, J. Stat. Phys. **65**, 715 (1991).

[52] G. G. Naumis, Phys. Rev. B **59**, 11315 (1999).

[53] E. Maciá, F. Triozon, and S. Roche, Phys. Rev. B **71**, 113106 (2005).

[54] D. Porath, A. Bezryadin, S. de Vries, and C. Dekker, Nature (London) **403**, 635 (2000); K. H. Yoo, D. H. Ha, J. O. Lee, J. W. Park, J. Kim, J. J. Kim, H. Y. Lee, T. Kawai, and H. Y. Choi, Phys. Rev. Lett. **87**, 198102 (2001); J. S. Hwang, K. J. Kong, D. Ahn, G. S. Lee, D. J. Ahn, and S. W. Hwang, Appl. Phys. Lett. **81**, 1134 (2002).

[55] H. Cohen, C. Nogues, R. Naaman, and D. Porath, Proc. Natl. Acad. Sci. U.S.A. **102**, 11589 (2005); J. Hihath, B. Xu, P. Zhang, and N. J. Tao, *ibid.* **102**, 16979 (2005).

[56] J. Yi, Phys. Rev. B **68**, 193103 (2003).

[57] A. J. Storm, J. van Noort, S. de Vries, and C. Dekker, Appl. Phys. Lett. **79**, 3881 (2001); Y. Zhang, R. H. Austin, J. Kraeft, E. C. Cox, and N. P. Ong, Phys. Rev. Lett. **89**, 198102 (2002); B. Hartzell, B. Melord, D. Asare, H. Chen, J. J. Heremans, and V. Sughomonian, Appl. Phys. Lett. **82**, 4800 (2003).

[58] E. G. Emberly and G. Kirczenow, Phys. Rev. B **58**, 10911 (1998).

[59] Y. A. Berlin, M. L. Burin, and M. A. Ratner, Superlattices Microstruct. **28**, 241 (2000); Y. Zhu, C. C. Kaun, and H. Guo, Phys. Rev. B **69**, 245112 (2004).

[60] E. Maciá, Nanotechnology **16**, S254 (2005).

[61] E. Maciá and F. Domínguez-Adame, *Electrons, Phonons and*

*Excitons in Low Dimensional Aperiodic Systems*, Colección Línea 300 (Editorial Complutense, Madrid, 2000).

[62] The role of contacts in the transmission efficiency through a metal-polyGACT-metal junction has been discussed in detail in Ref. 53.

[63] R. Gutiérrez, D. Porath, and G. Cuniberti, in *Charge Transport in Disordered Solids with Applications in Electronics*, edited by S. Baranovski (Wiley, Hoboken, NJ, 2006).

[64] R. Gutiérrez, S. Mandal, and G. Cuniberti, Phys. Rev. B **71**, 235116 (2005); Nano Lett. **5**, 1093 (2005); A. Nitzan, J. Phys. Chem. A **105**, 2677 (2001).

[65] S. Roche, Phys. Rev. Lett. **91**, 108101 (2003).

[66] R. A. Caetano and P. A. Schulz, Phys. Rev. Lett. **95**, 126601 (2005); **96**, 059704 (2006).

[67] A. Sedrakyan and F. Domínguez-Adame, Phys. Rev. Lett. **96**, 059703 (2006); E. Díaz, A. Sedrakayan, D. Sedrakayan, and F. Domínguez-Adame, cond-mat/0605403, Phys. Rev. B (to be published).

[68] Z. Kutnjak, C. Filipič, R. Podgornik, L. Nordenskiöld, and N. Korolev, Phys. Rev. Lett. **90**, 098101 (2003).

[69] Z. G. Yu and X. Song, Phys. Rev. Lett. **86**, 6018 (2001).

[70] P. Tran, B. Alavi, and G. Gruner, Phys. Rev. Lett. **85**, 1564 (2000).

[71] K. H. Yoo, D. H. Ha, J. O. Lee, J. W. Park, J. Kim, J. J. Kim, H. Y. Lee, T. Kawai, and H. Y. Choi, Phys. Rev. Lett. **87**, 198102 (2001).

[72] S. S. Alexandre, E. Artacho, J. M. Soler, and H. Chacham, Phys. Rev. Lett. **91**, 108105 (2003).

[73] W. Zhang, A. O. Govorov, and S. E. Ulloa, Phys. Rev. B **66**, 060303(R) (2002).

[74] G. P. Triberis, C. Simserides, and V. C. Karavolas, J. Phys.: Condens. Matter **17**, 2681 (2005).